Bioorganic & Medicinal Chemistry Letters 19 (2009) 4832–4835

Contents lists available at ScienceDirect

Bioorganic & Medicinal Chemistry Letters

journal homepage: www.elsevier.com/locate/bmcl

Novel inhibitors of the αvβ3 integrin—lead identification strategy

David Elliot, Eleanor Henshaw, Philip A. MacFaul, Andrew D. Morley *, Peter Newham, Keith Oldham, Ken Page, Neil Rankine, Paul Sharpe, Attilla Ting *, Christine M. Wood

AstraZeneca, Mereside, Alderley Park, Macclesfield, Cheshire SK10 4TG, UK

ARTICLE INFO

Article history:
Received 3 April 2009
Revised 8 June 2009
Accepted 10 June 2009
Available online 13 June 2009

Keywords:
Integrin
Inhibitor
Lead identification

ABSTRACT

A novel approach to inhibition of the αvβ3 integrin is described, which uses compounds designed to generate nM potency without using the arginine binding site.

Integrins are a family of cell surface heterodimeric adhesion receptors composed of α and β chains. Ligands include cell surface counter receptors (e.g., the cell adhesion molecules or CAMs), ligands of the vasculature (e.g., fibrinogen) and extracellular matrix macromolecules (e.g., collagens and fibronectin). Integrin–ligand interactions are critical for cell positioning within tissues, for providing traction and guidance during cell migration, for mechanotransduction and for the organization of signaling complexes that modulate cell phenotype.[1]

αvβ3 acts as a regulator of disease pathology associated with cancer, osteoporosis and rheumatoid arthritis.[2–4] For example, endothelial cell αvβ3 regulates the survival of angiogenic vessels, osteoclast αvβ3 supports firm adhesion to the bone matrix, facilitating bone remodeling, while macrophage αvβ3 appears to play a role in modulating pro-inflammatory cytokine expression.

Although numerous small molecule ligands of αvβ3 are known,[5,6] all contain motifs that mimic the arginine and aspartate of the RGD tripeptide, present in endogenous protein ligands. Whilst these zwitterionic inhibitors provide potency, they are frequently large, and highly flexible, invariably leading to sub-optimal in vivo pharmacokinetic profiles. Although a significant number of small molecule antagonist structures have been published for this target, very few compounds have progressed into clinical development. At the outset of our work we decided to follow an alternative antagonist development approach. The carboxylate present in all known αvβ3 inhibitors mimics the acidic moiety of the RGD tripeptide and thus competes with physiological ligands. These acid motifs coordinate the Mg^{2+} present in the metal ion adhesion site (MIDAS) located within the integrin β subunit, while the arginine side chain of physiological ligands inserts into a narrow groove on the α subunit. Our hit identification strategy was to identify αvβ3 MIDAS-binders that achieved high binding affinity through alternative interactions on the αβ interface. The strategy is depicted schematically in Figure 1. Thus our hit-finding approach centered on a directed screen of low molecular weight carboxylic acids and isosteres (MW <350).

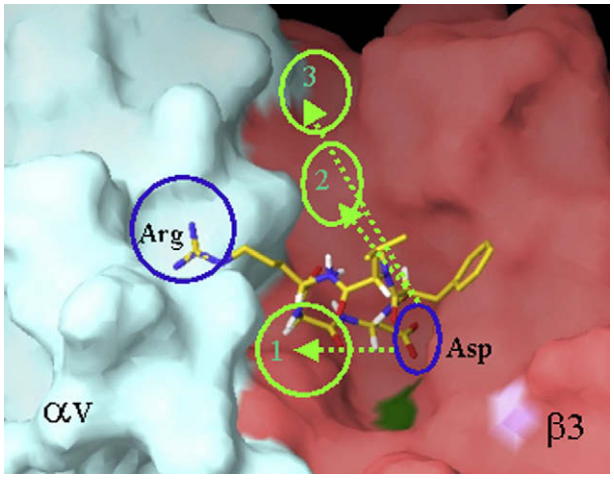

Figure 1. CycloRGDFV bound to αvβ3[13] (RCSB code:1L5G). Carboxylate and arginine motifs are circled in blue. The strategy is to explore potential binding sites (green circles 1–3) at the interface of the integrin dimer.

* Corresponding authors.
E-mail address: andy.morley@astrazeneca.com (A.D. Morley).

0960-894X/$ - see front matter © 2009 Elsevier Ltd. All rights reserved.
doi:10.1016/j.bmcl.2009.06.041

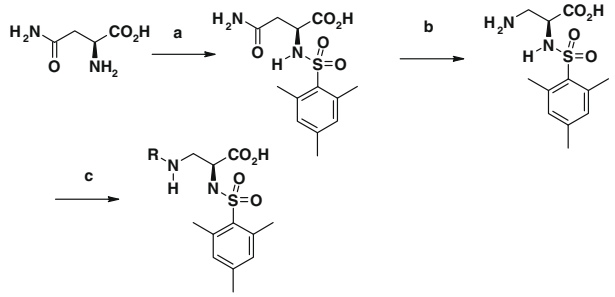

Scheme 1. Reagents: (a) mesityl chloride, NaOH, dioxane; (b) Br_2, NaOH/H_2O; (c) HATU, acid, DMF, DIPEA or chlorofomate, DIPEA, THF, or PhCHO, $NaCNBH_3$, AcOH, MeOH/CH_2Cl_2.

The strength of this approach is that it has the potential to identify novel scaffolds with superior pharmacokinetic profiles over standard RGD mimics. However, since it is unclear if alternative binding modes are consistent with high affinity interactions, there was a risk that compounds of this type may only possess modest potency.

One of the hits from screening was **1**, which had an IC50 of 800 nM in inhibiting fibrinogen binding to αvβ3 and was used as the start point for lead identification.

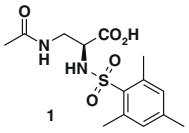

1

The synthesis of **1** and analogues is outlined in Scheme 1. This was achieved using commercial R-asparagine as a start point, following known literature procedures.[7]

Preliminary derivatization focused on the exploration of the SAR around the acetamide motif of **1**. Data for key compounds is highlighted below in Table 1.

Most modifications in this region dramatically reduced potency. The removal of the acetyl (**2**) or its replacement with methyloxycarbonyl (**5**) or methylsulfonyl (**6**) completely abolished αvβ3 activity. Further derivatization of the amide was specific, 3-methlypropanoyl (**3**) losing >30-fold activity and most other modifications being inactive. The only positive variation was the incorporation of a benzoyl motif (**7**) which increased potency by ~7-fold. Expansion of these results showed that the addition of a linker between the aromatic and the amide (**8**) or the removal of the carbonyl (**9**) significantly reduced potency.

Table 1
SAR of the acetamide

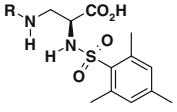

Compd	R	αvβ3IC$_{50}$[a] (μM)
1	Acetyl	0.8
2	Hydrogen	>50
3	3-Methlypropanoyl	30
4	*tert*-Butyloxycarbonyl	>50
5	Methyloxycarbonyl	>50
6	Methylsulfonyl	>50
7	Benzoyl	0.12
8	2-Phenylacetyl	>50
9	Benzyl	>50

[a] Values are means of three experiments.

Table 2
SAR of the α-amino motif

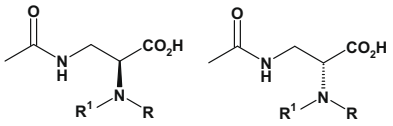

R isomer S isomer

Compd	Isomer	R	R^1	αvβ3 IC_{50} (μM)
1	R	(2,4,6-Trimethylphenyl)sulfonyl	H	0.8
10	S	(2,4,6-Trimethylphenyl)sulfonyl	H	8
11	R	Phenylsulfonyl	H	9.1
12	R	Benzylsulfonyl	H	>50
13	R	Benzoyl	H	>50
14	R	2,6-Dichlorobenzoyl	H	>50
15	R	Phenoxycarbonyl	H	>50
16	R	*tert*-Butyloxycarbonyl	H	>50
17	R	(2,4,6-Trimethylphenyl)sulfonyl	Me	>50

In parallel to the work above, the initial exploration of the SAR around the α-amino substituent was also undertaken and is shown in Table 2.

The R enantiomer (**1**) of the amino acid is 10-fold more potent than the S (**10**). The removal of the methyl substituents from the aromatic ring of the sulfonamide (**11**) also resulted in a 10-fold loss of potency. Further derivatization of the molecule in this region by replacement of the sulfonamide with small sub sets of amides and carbamates abolished activity in all cases, as did methylation of the sulfonamide (**17**).

As the benzamide analogues are truncated versions of known integrin inhibitors,[5,6,8,9] a library of aromatic amide analogues, based on (**7**) was synthesized and tested to explore the SAR in more detail. Data for key compounds is shown in Table 3.

A variety of aromatic rings can be incorporated in this region, the majority maintaining potency in the 10–300 nM range. Further derivatization is tolerated. SAR can be quite specific, but no significant increase in potency was observed through elaboration with additional substituents.

Compounds **18** and **25** are a matched pair, showing that larger motifs are tolerated, but result in loss of potency (~8-fold). The modeling of known RGD mimetics and project compounds support the observed SAR.[10] The overlay of L739758[11,12] into the αvβ3 crystal structure[13] suggests that the carboxylate binds to the MIDAS site, along with the sulfonamide oxygen and nitrogen forming H-bonds to backbone amides. The basic piperidine extends towards to the alpha subunit, forming another H-bond. The central portion of the molecule acts purely as a spacer that links the molecular fragments that bind into the α and β subunits. Modeling suggested

Table 3
SAR of the aromatic amide

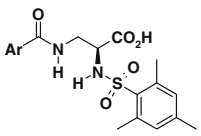

Compds	Ar	αvβ3 IC_{50} (nM)
18	3-Thienyl	44
19	3-Furyl	32
20	2-Methylpyrazol-3-yl	11
21	2-Methyloxazol-4-yl	41
22	3-Pyridyl	81
23	5-Pyrimidinyl	63
24	4-Pyridyl	301
25	Benzo[*b*]thiophene	350

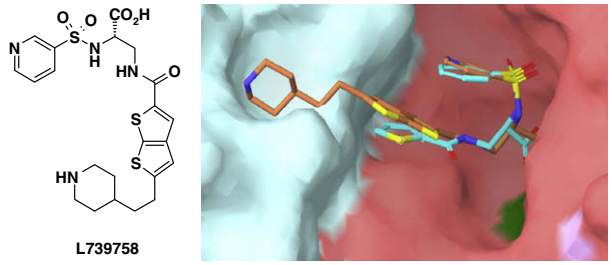

Figure 2. Overlay of Merck compound L739758[11,12] in orange (RCSB code: 1TY7) and potential binding mode of compound 18 (cyan) in αvβ3 crystal[13] (RCSB code: 1L5G), showing molecular surface of the protein.

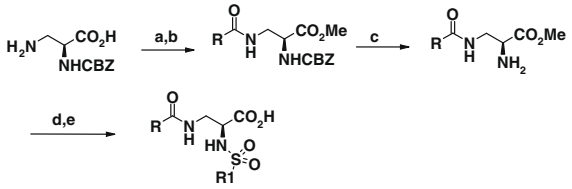

Scheme 2. Reagents: (a) $SOCl_2$, MeOH; (b) HATU, acid, CH_2Cl_2, DIPEA; (c) HBr, AcOH; (d) sulfonyl chloride, DIPEA, CH_2Cl_2; (e) 1 M NaOH, MeOH.

that the benzo[*b*]thiophene of **25** can bind in a similar manner to the thienothiophene ring in L739758, while the thiophene analogue (**18**) is small enough to bind more deeply into the hydrophobic grove and make additional interactions with the protein, as shown in Figure 2. Further analysis of the predicted binding mode of **18** indicated that the carboxylate would bind to the MIDAS site while the sulfonamide would form an H-bond to the backbone as observed in L739758. The amide orientation of **18** overlays well with the crystal structure of cyclo RGD mimetics, and positions the thiophene into the hydrophobic grove.

Fixing the amide substituent as phenyl, 3-thienyl and 3-furyl, initial evaluation of the SAR around the sulfonamide was undertaken. Compounds were synthesized as highlighted in Scheme 2 and SAR is detailed in Table 4.

Lipophilic motifs were preferred at the ortho position of Ar_2. The addition of a second ortho substituent did not offer any significant improvement in potency. The incorporation of functionality in the 3 and 4-positions was encouraging with a diverse set of analogues tolerated. Variations around the sulfonamide were generally consistent with any changes to Ar_1.

The series showed promising potency without an arginine mimetic and key compounds were profiled more widely (Table 5). Physicochemical and in vitro DMPK profiles are encouraging for Lead Identification.

Compound **21** was evaluated in a rat PK study and found to have an iv clearance of 4.7 ml/min/kg, a V_{dss} of 0.8 l/kg and a terminal $T_{1/2}$ of 7 h. Oral dosing showed it to have bioavailability of 15%. Whilst this is a modest profile, it appears to be superior to the related diaminopropionic acid templates which incorporate an arginine mimic.[14] Bioavailability appears to be permeability limited, as **21** possesses solubility in excess of 1 mM, whilst PAMPA experiments showed a P_{app} value of 0.1×10^6 cm/s. This lies just within the low permeability classification (<30% predicted F_{abs}) as defined by internal validation data comparing human F_{abs} and P_{app} for a set of around 70 oral drugs.[15] In an attempt to increase the inherent series permeability, we explored modification of the amide in more detail. Results are detailed in Table 6.

The replacement on the secondary amide (**19**) with a tertiary analogue (**39**) maintained a similar lipophilicity value (*clog P*), enhanced permeability by threefold (PAMPA), but lost >300-fold in potency. This is supported by modeling, where the tertiary amide would clash with the furan ring, unless a different amide orientation is adopted. The five-membered lactam (**40**) also lost activity, but not as dramatically, presumably because it is conformationally constrained. The incorporation of an ortho methoxy substituent (**41**) slightly increased αvβ3 activity, compared to **7**, whilst sub-

Table 4
SAR of the sulfonamide

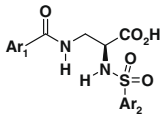

Compds	Ar_1	Ar_2	αvβ3 IC_{50} (nM)
26	Phenyl	o-Tolyl	320
27	Phenyl	2-Chlorophenyl	260
28	Phenyl	2-Iodophenyl	25
29	Phenyl	2-Methylsulfonylphenyl	4600
30	Phenyl	2-Methoxyphenyl	729
31	Phenyl	2,3-Dichlorophenyl	62
32	Phenyl	2,6-Dichlorophenyl	118
33	3-Thienyl	2,3-Dichlorophenyl	19
34	3-Thienyl	2,4-Dichlorophenyl	8
35	3-Thienyl	2,4,6-Trichlorophenyl	24
36	3-Furyl	3-Cyanophenyl	98
37	3-Furyl	3-Methoxyphenyl	208
38	3-Furyl	3-Pyridyl	793

Table 5
Profiles of key lead generation compounds

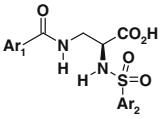

Compd	**20**	**21**	**33**
Ar_1	2-Methylpyrazol-3-yl	2-Methyloxazol-4-yl	3-Thienyl
Ar_2	(2,4,6-Trimethyl-phenyl)sulfonyl	(2,4,6-Trimethyl-phenyl)sulfonyl	2,3-Dichloro-phenyl
αvβ3IC50 (nM)	11	41	19
Mol Wt (g/mol)	394	395	423
Solubility (μM)	>3000	>2000	>3000
Rat PB (% free)	16.6	4.9	2.7
Log *P*	1.85	1.5	2
Rat heps (μl/min/10^6 cells)	12.5	4.8	9.9
Hu mics (μl/min/mg)	14.6	4.7	<2
Cyp (μM)	>10 (5/5)	>10 (5/5)	>10 (5/5)
PAMPA (10^6 cm/s)	0.021	0.1	0.046

Table 6
Effect of amide modification

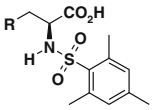

Compd	R	αvβ3 IC_{50} (nM)	*clog P*	PAMPA (10^6 cm/s)
19	Furan-3-carbonylamino	32	1.9	0.14
39	Furan-3-carbonyl-methyl-amino	8000	1.98	0.45
7	Benzamido	120	2.5	0.15
40	1-Oxoisoindolin-2-yl	975	2.1	0.8
41	2-Methoxybenzamide	78	2.5	4.6

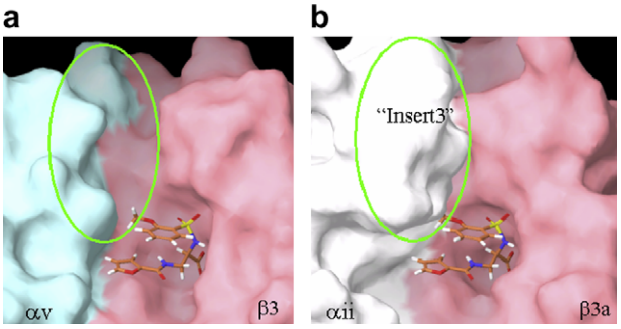

Figure 3. (a) Binding mode of compound **43** (cyan) in αvβ3 crystal (RCSB code: 1L5G). (b) Overlay binding mode of compound **43** (cyan) into αiiβ3a crystal (RCSB code: 1TY7).

Table 7
Selectivity comparisons

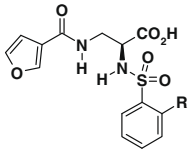

Compd	R	αvβ3 IC_{50} (nM)	αiiβ3a IC_{50} (nM)
42	Me	260	2380
43	OMe	700	>100,000

stantially increasing the overall permeability, making this a useful observation to develop further.

Disappointingly, most analogues showed only modest selectivity for αvβ3 over αiiβ3a (5–10-fold). Analysis of the X-ray structures showed differences in the regions highlighted in Figure 3, and modeling suggested that the ortho position of the sulfonamide might be a good area to target to improve selectivity. Broader testing of ortho substituted analogues highlighted the following matched pair comparison (Table 7).

Compound **43** demonstrates >130-fold selectivity for αvβ3 over αiiβ3a. This improvement in selectivity can be rationalized by the presence of 'insert 3'[11,12] in αii. This significantly modifies the interface for αiiβ3a compared to αvβ3 in this region and also restricts the conformational freedom of Tyr 190. Modeling[10] suggest the 2-methoxy substituent of compound **43** (Fig. 3b) will be positioned unfavorably close to Tyr190 in αii, whilst the absence of 'insert3' and subsequent differing conformation of Tyr 178 in αv is tolerated.

This approach described above demonstrates that for αvβ3, low nM potency is achievable without the need to incorporate an arginine mimetic. The observed SAR and overall profiles of the compounds produced in Lead Generation are different from those previously published for this target. Broader SAR exploration of target areas 2 and 3 of Figure 1 through derivatizing the ortho position of the sulfonamide should improve selectivity and possibly potency and would form the key strategy for Lead Optimization.

Acknowledgement

The authors would like to acknowledge the input and advice of Dr. Peter Kenny in the preparation of this Letter.

References and notes

1. Hynes, R. O. *Cell* **2002**, *110*, 673.
2. Cai, W.; Chen, X. *Anticancer Agents Med. Chem.* **2006**, *6*, 407.
3. Nakamura, I.; Duong, le T.; Rodan, S. B.; Rodan, G. A. *J. Bone Miner. Metab.* **2007**, *25*, 337.
4. Wilder, R. L. *Ann. Rheum. Dis.* **2002**, *61*(Suppl 2), ii96.
5. Coleman, P. J.; Duong, Le T. *Expert Opin. Therapeutic Patent* **2002**, *12*, 1009.
6. Henry, C.; Moitessier, N.; Chapleur, Y. *Mini-Rev. Med. Chem.* **2002**, *2*, 531.
7. Jones, R. C. F.; Dickson, J. *J. Pept. Sci.* **2000**, *6*, 621.
8. Kubota, D.; Ishikawa, M.; Yamamoto, M.; Murakami, S.; Hachisu, M.; Katano, K.; Ajito, K. *Bioorg. Med. Chem.* **2006**, *14*, 2089.
9. Duggan, M. E.; Duong, L. T.; Fisher, J. E.; Hamill, T. G.; Hoffman, W. F.; Huff, J. R.; Ihle, N. C.; Leu, C.-T.; Nagy, R. M.; Perkins, J. J.; Rodan, S. B.; Wesolowski, G.; Whitman, D. B.; Zartman, A. E.; Rodan, G. A.; Hartman, G. D. *J. Med. Chem.* **2000**, *43*, 3736.
10. Models of the binding modes of compounds **18**, **25** and **43** with αvβ3 were generated from the RCSB (home.rcsb.org) Protein Data Bank (www.rcsb.org/pdb/home/home.do), with entry reference code 1L5G (Ref. 13) using the Maestro molecular modeling program. The models were docked using Glide and then energy-minimized using OPLS 2005 force field. Glide, Maestro and MarcoModel were licensed from Schrödinger, LGG (www.schrodinger.com).
11. Xiao, T.; Takagi, J.; Coller, B. S.; Wang, J.-H.; Springer, T. A. *Nature*, 2004. 59.
12. Since completion of the work described above, a re-refinement of the L-739758 in αiiβ3a complex has been deposited in the RCSB PDB with Refcode: 2vc2 replacing the previous version Refcode: 1TY7 (the coordinates are still available). There are subtle difference observed between the two versions, but this did not impact significantly on our findings and our strategy going into Lead Optimization.
13. Xiong, J-P.; Stehle, T.; Zhang, R.; Joachimiak, A.; Frech, M.; Goodman, S. L.; Arnaout, M. A. *Science* **2002**, *296*, 151.
14. Ishikawa, M.; Hiraiwa, Y.; Kubota, D.; Tsushima, M.; Watanabe, T.; Murakami, S.; Ouchi, S.; Ajito, K. *Bioorg. Med. Chem.* **2006**, *14*, 2131.
15. Unpublished AstraZeneca data.